

Bulk Electronic structure of $\text{Na}_{0.35}\text{CoO}_2 \cdot 1.3\text{H}_2\text{O}$

A. Chainani,¹ T. Yokoya,² Y. Takata,¹ K. Tamasaku,³ M. Taguchi,¹ T. Shimojima,² N. Kamakura,¹ K. Horiba,¹ S. Tsuda,² S. Shin,^{1,2} D. Miwa,³ Y. Nishino,³ T. Ishikawa,³ M. Yabashi,⁴ K. Kobayashi,⁴ H. Namatame,⁵ M. Taniguchi,⁵ K. Takada,^{6,7} T. Sasaki,^{6,7} H. Sakurai,⁶ and E. Takayama-Muromachi.⁶

¹*Soft X-ray Spectroscopy Lab, RIKEN/SPring-8,*

1-1-1 Kouto, Mikazuki-cho, Sayo-gun, Hyogo 679-5148, Japan

²*Institute for Solid State Physics, University of Tokyo, Kashiwa, Chiba 277-8581, Japan*

³*Coherent X-ray Optics Lab, RIKEN/SPring-8, 1-1-1 Kouto, Mikazuki-cho, Sayo-gun, Hyogo 679-5148, Japan*

⁴*JASRI/SPring-8, 1-1-1 Kouto, Mikazuki-cho, Sayo-gun, Hyogo 679-5198, Japan*

⁵*HiSOR, Hiroshima University, 2-313 Kagamiyama, Higashi-Hiroshima 739-8526, Japan*

⁶*National Institute for Materials Science, Tsukuba, Ibaraki, 305-0044, Japan and*

⁷*CREST, Japan Science and Technology Corporation*

(Dated: November 12, 2018)

High-energy ($h\nu = 5.95$ KeV) synchrotron Photoemission spectroscopy (PES) is used to study bulk electronic structure of $\text{Na}_{0.35}\text{CoO}_2 \cdot 1.3\text{H}_2\text{O}$, the layered superconductor. In contrast to 3-dimensional doped Co oxides, Co $2p$ core level spectra show well-separated Co^{3+} and Co^{4+} ions. Cluster calculations suggest low spin Co^{3+} and Co^{4+} character, and a moderate on-site Coulomb correlation energy $U_{dd} \sim 3\text{--}5.5$ eV. Photon dependent valence band PES identifies Co $3d$ and O $2p$ derived states, in near agreement with band structure calculations.

PACS numbers: 74.25.Jb, 74.25.Kc, 79.60.-i

The discovery of superconductivity in the hydrated Co oxide $\text{Na}_{0.35}\text{CoO}_2 \cdot 1.3\text{H}_2\text{O}$ is important in terms of a layered triangular lattice with superconductivity.¹ Since it has two-dimensional CoO_2 layers consisting of (CoO_6) octahedra and Na^{1+} content corresponds to Co^{3+} valency in a matrix of Co^{4+} ions, it is reminiscent of doping induced superconductivity as in high- T_c cuprates. In spite of extensive investigations,² it has not been possible to achieve superconductivity in a 3-dimensional Co-oxide system. Electron-electron correlations between Co $3d$ electrons is believed to be substantial (on-site Coulomb energy, $U_{dd} = 3\text{--}5.5$ eV) from electron spectroscopic studies,^{3,4,5,6,7} albeit less than copper oxides ($U_{dd} = 5\text{--}8$ eV, Ref. 8). Theoretical studies,^{9,10,11,12} including resonating-valence-bond models, predict fascinating properties for this system. Recent experiments signifying strong correlations show dimensional crossover¹³ and the relation of spin entropy with the large thermopower¹⁴ in the non-superconducting compositions.

From the point of conventional phonon-mediated superconductivity, weak or strong electron-phonon coupling leading to superconductivity also needs to be carefully investigated for the Co-oxide superconductors. This is because the doping dependent T_c 's are rather low,¹⁵ with a maximum T_c of ~ 5 K. The layered Co oxides thus provide a new opportunity to study charge and spin dynamics in superconducting oxides. Recent studies indicate that Na_xCoO_2 is close to charge and spin ordering tendencies.^{16,17} NMR studies¹⁸ on non-superconducting Na_xCoO_2 have concluded integral valent Co^{3+} and Co^{4+} ions reflecting charge order. Also, while intercalated water is necessary for superconductivity, its role in modifying the electronic structure is not yet clear. It is thus important to study the electronic structure of $\text{Na}_x\text{CoO}_2 \cdot y\text{H}_2\text{O}$ as a function of Na content,

x and water content, y.

Photoemission spectroscopy (PES) has provided a systematic enumeration of the electronic structure of transition metal compounds^{3,4,5,6,7,8} based on the Zaanen-Sawatzky-Allen (ZSA) phase diagram.¹⁹ Core-level PES provides valence states and a reasonable estimate of electronic structure parameters : on-site Coulomb energy (U_{dd}), charge-transfer (CT) energy (Δ) and hybridization strength (V). Further, while angle-resolved (AR) valence band (VB) PES is necessary to study experimental band structure, angle integrated VB-PES provides the transition probability modulated density of states (DOS). The surface sensitivity of PES has often led to controversies regarding surface *vis'* - *a* - *vis'* bulk electronic structure, and hence, high-energy (HE)-PES as well as site-selective PES are very important and promising.^{20,21} A recent development using a high-throughput fixed photon energy and a resolution of 240 meV at a kinetic energy of 5.95 KeV, is a valuable advance for investigating bulk electronic structure of materials.²² Its efficacy was demonstrated for a high-K dielectric material for semiconductor applications.²² The principal advantage of HE-PES is the high escape depth of emitted photoelectrons,²³ enabling a truly bulk measurement. At $h\nu = 5.95$ KeV, the escape depth for Co $2p$ and O $1s$ electrons is estimated to be ~ 50 Å, significantly higher than that with soft x-ray photons from a Mg- or Al- $K\alpha$ source (~ 10 Å).²³ Since photo-ionization cross sections (PICS) become very low at high photon energies,²⁴ VB studies at $h\nu \geq 5$ keV were very difficult earlier, although the first core level study using 8 KeV photons was done nearly 30 years ago.²⁵

We study VB and core-level HE-PES ($h\nu = 5.95$ KeV) of the Co oxide superconductor, $\text{Na}_{0.35}\text{CoO}_2 \cdot 1.3\text{H}_2\text{O}$ and non-superconducting $\text{Na}_{0.7}\text{CoO}_2$. Co $2p$ core level spec-

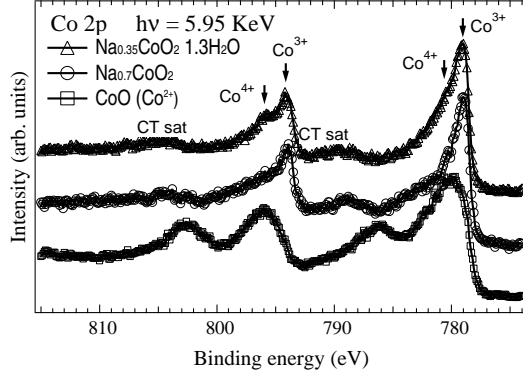


FIG. 1: Co 2p core level PES spectra of $\text{Na}_{0.35}\text{CoO}_2 \cdot 1.3\text{H}_2\text{O}$, $\text{Na}_{0.7}\text{CoO}_2$ and CoO obtained using $h\nu = 5.95$ KeV photons.

tra show well defined Co^{3+} and Co^{4+} features in the normal phase of $\text{Na}_{0.35}\text{CoO}_2 \cdot 1.3\text{H}_2\text{O}$. Cluster calculations indicate a moderate $U_{dd} \sim 3\text{-}5.5$ eV. The O $1s$ spectrum of $\text{Na}_{0.35}\text{CoO}_2 \cdot 1.3\text{H}_2\text{O}$ shows a two-peak structure due to signals from CoO_2 layers and water, respectively. The VB spectra consisting of Co $3d$ and O $2p$ derived states are compared with soft x-ray ($h\nu = 700$ eV) PES and reported band structure calculations (BSCs). The VB is similar for both compositions on the energy scale of the resolution used, suggesting important modifications only at a lower energy scale near the Fermi level (E_F),¹³ probably related to confined carriers in CoO_2 layers and/or a modified electron-phonon coupling.

Polycrystalline samples of $\text{Na}_{0.35}\text{CoO}_2 \cdot 1.3\text{H}_2\text{O}$ and $\text{Na}_{0.7}\text{CoO}_2$ were made and characterized as described in Ref. 1. Magnetization measurements confirmed the bulk T_c of 4.5 K for $\text{Na}_{0.35}\text{CoO}_2 \cdot 1.3\text{H}_2\text{O}$. To ensure retention of water under vacuum conditions, freshly prepared samples were mounted on substrates with silver paste and also covered with it. After transferring samples to the measurement chamber and cooling to 100 K, they were scraped in-situ with a diamond file to obtain clean surfaces. The samples were then cooled to 15 K for HE-PES measurements, at a vacuum of 1×10^{-10} Torr. HE-PES was performed at undulator beam line BL29XU, Spring-8 (Ref. 26) using 5.95 KeV photons and a modified SES2002 electron analyzer. The energy width of incident x-rays was 70 meV, and the total energy resolution, ΔE was set to ~ 0.5 eV. Soft x-ray PES ($h\nu = 700$ eV) was performed at BL19B, KEK, PF, using a CLAM4 electron analyzer with $\Delta E \sim 0.3$ eV. Samples were cooled to 30 K and the vacuum was 8×10^{-10} Torr during measurements. Single crystal CoO was scraped in-situ and measured at 300 K to calibrate the energy scale. E_F of gold was also measured to calibrate the energy scale.

Figure 1 shows the Co $2p$ core level PES spectra of $\text{Na}_{0.35}\text{CoO}_2 \cdot 1.3\text{H}_2\text{O}$, $\text{Na}_{0.7}\text{CoO}_2$ and CoO obtained using $h\nu = 5.95$ KeV photons. The Co 2p spectrum of $\text{Na}_{0.35}\text{CoO}_2 \cdot 1.3\text{H}_2\text{O}$ exhibits main peaks derived from Co $2p_{3/2}$ and $2p_{1/2}$ due to spin-orbit splitting, and two small humps or satellites at ~ 10 eV higher binding energy (BE) from the main peaks. The $2p_{3/2}$ peak itself

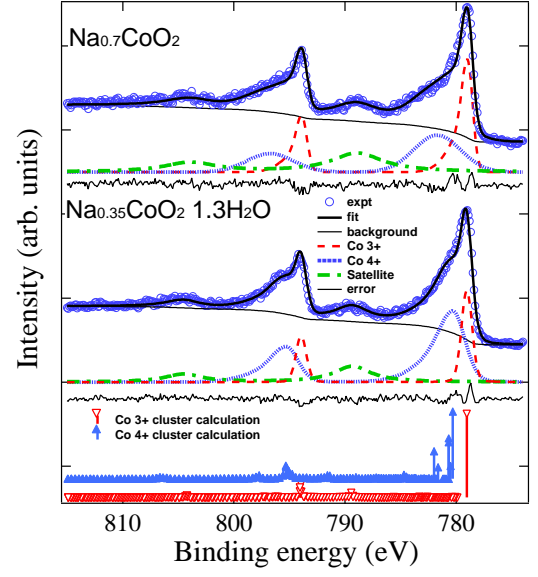


FIG. 2: (Color online) A least-squares curve-fit to the Co 2p spectrum of $\text{Na}_{0.35}\text{CoO}_2 \cdot 1.3\text{H}_2\text{O}$ and $\text{Na}_{0.7}\text{CoO}_2$, shows contributions of Co^{3+} and Co^{4+} states in the $2p_{3/2}$ and $2p_{1/2}$ main peaks, with a single peak assumed for satellites. Line diagrams show calculated low-spin Co^{3+} and Co^{4+} states.

consists of two peaks. This is clear in the $2p_{1/2}$ region with well-separated peaks in raw spectra. A simple interpretation is that the low BE peak is due to Co^{3+} and the high BE peak is due to Co^{4+} states. In Fig. 2 we overlay a least-squares curve fit on the data of $\text{Na}_{0.35}\text{CoO}_2 \cdot 1.3\text{H}_2\text{O}$ and $\text{Na}_{0.7}\text{CoO}_2$, obtained using asymmetric Voigt functions and a Shirley background. The fits resolve contributions of Co^{3+} and Co^{4+} features in the main peaks, as seen in the decomposition. We used a single feature for the satellites for simplicity. The peak widths for Co^{4+} feature and satellite in $\text{Na}_{0.7}\text{CoO}_2$ are broader than in $\text{Na}_{0.35}\text{CoO}_2 \cdot 1.3\text{H}_2\text{O}$, suggesting larger inhomogeneity in valency due to increased Na doping. The crystal structure analysis of both samples indicated absence of impurity phases within experimental accuracy. Further, we have carefully checked that BE's for Co^{3+} main peaks are actually lower than the corresponding peaks of Co^{2+} in CoO, e.g. $2p_{3/2}$ peak is at 779.0 eV and 780.0 eV, respectively (Fig. 1). The CoO spectra match those obtained with a $\text{MgK}\alpha$ source extremely well in BE and spectral shapes.^{3,7} Well-separated core-level features are observed in classic non-oxide charge-density wave (CDW) systems²⁷ as well as intermediate valence materials without static charge order²⁸, because PES is a fast probe. Earlier work on 3-dimensional perovskite oxides $\text{La}_{1-x}\text{Sr}_x\text{CoO}_3$ ($x = 0.0\text{-}0.4$) showed essentially a single peak at the same BE, and no clear separation into Co^{3+} and Co^{4+} states.^{4,5} The peak width broadened initially with doping for $x = 0.1$, but across the semiconductor-metal transition at $x = 0.2$ in $\text{La}_{1-x}\text{Sr}_x\text{CoO}_3$, the peaks became narrower for increasing x due to uniform non-integral valency at Co-

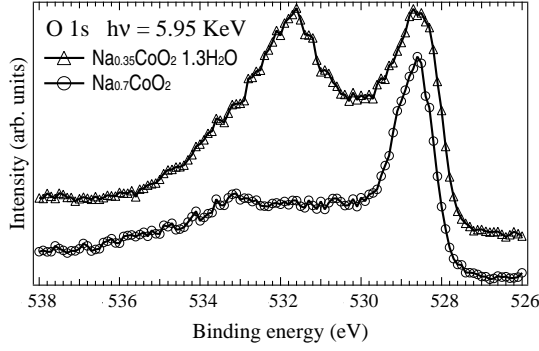


FIG. 3: O $1s$ core level PES spectra of $\text{Na}_{0.35}\text{CoO}_2 \cdot 1.3\text{H}_2\text{O}$ and $\text{Na}_{0.7}\text{CoO}_2$ obtained using $h\nu = 5.95$ KeV photons, showing the presence of water derived O $1s$ signal in superconducting composition.

sites.⁴ In misfit layered Co-oxides (BiPb)Sr-Co-O with an average valence of 3.33 and 3.52, no clear Co^{4+} separated from Co^{3+} was concluded.⁶ Surprisingly, for oxide systems which show charge-ordering or disproportionation, such as $\text{Pr}_{0.5}\text{Sr}_{0.5}\text{MnO}_3$, perovskite ferrites, etc. well-separated integral valence features are not observed.^{29,30} It is due to the ground state being dominated by a CT $d^{n+1}L^1$ (L is a ligand hole) rather than a d^n configuration, based on model Hamiltonian cluster calculations.³⁰ From similar cluster calculations (details are described in Ref. 30 and results of one such calculation for low spin Co^{3+} and Co^{4+} are shown as line diagrams in Fig. 2), we obtain the electronic structure parameters of $U_{dd} = 5.5$ eV, $\Delta = 4.0$ eV and $V = 3.1 \pm 0.2$ eV which describe the Co $2p$ spectral features fairly well. For simplicity, we use the same parameter values for Co^{3+} and Co^{4+} except for crystal field splitting, $10Dq$. The $10Dq$ values for Co^{3+} and Co^{4+} are 2.5 eV and 4.0 eV, respectively. The uncertainty in Δ is ± 0.5 eV while the calculated spectra were very similar for $U_{dd} = 3.0$ -5.5 eV, consistent with earlier work.^{3,4,5,6,7} The ground state character for Co^{3+} is $3d^6 = 57.0\%$, $3d^7L^1 = 38.1\%$ and $3d^8L^2 = 4.9\%$, while that for Co^{4+} is $3d^5 = 57.4\%$, $3d^6L^1 = 37.6\%$ and $3d^7L^2 = 5.0\%$. We have also checked for high-spin Co^{3+} and Co^{4+} configurations but the results are not compatible with the data. The analysis suggests that $\text{Na}_{0.35}\text{CoO}_2 \cdot 1.3\text{H}_2\text{O}$ and $\text{Na}_{0.7}\text{CoO}_2$ contain low spin Co^{3+} and Co^{4+} configurations, consistent with magnetic measurements.¹⁷ The calculations also show CT character of the satellites. The results indicate an electronic structure of mixed character, but more Mott-Hubbard-like rather than CT-like in terms of the ZSA phase diagram.

While the main peaks of Co^{3+} and Co^{4+} features are well-separated, it is clear from the cluster calculations that Co $2p$ spectra consist of degenerate multiple features at higher BEs. The satellite intensity is also large, being $\sim 70\%$ of the Co^{3+} main peak. It is hence difficult to estimate the actual $\text{Co}^{3+} : \text{Co}^{4+}$ relative concentrations although the main peak intensities are roughly consistent (within 10 %) of the nominal concentrations. The present studies are consistent with in-

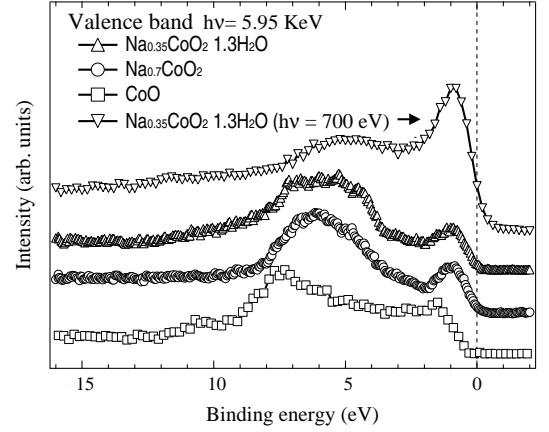


FIG. 4: Valence band HE-PES ($h\nu = 5.95$ KeV) spectra of $\text{Na}_{0.35}\text{CoO}_2 \cdot 1.3\text{H}_2\text{O}$, $\text{Na}_{0.7}\text{CoO}_2$ and CoO, and of $\text{Na}_{0.35}\text{CoO}_2 \cdot 1.3\text{H}_2\text{O}$ obtained using $h\nu = 700$ eV photons. The Co $3d$ states are enhanced in the $h\nu = 700$ eV spectrum.

tegral valent charge order measured by NMR studies.¹⁸ Although LDA + U calculations¹⁶ for $\text{Na}_{0.33}\text{CoO}_2$ indicate a correlation driven charge order with a ferromagnetic ground state, the absence of ferromagnetic order and suppression of Co moments on introducing water in $\text{Na}_{0.35}\text{CoO}_2 \cdot 1.3\text{H}_2\text{O}$ (Ref. 32) suggests an additional input to the electronic structure, most likely strong electron-phonon coupling as in regular CDW transitions.

The O $1s$ core level HE-PES spectra of $\text{Na}_{0.35}\text{CoO}_2 \cdot 1.3\text{H}_2\text{O}$ and $\text{Na}_{0.7}\text{CoO}_2$ are shown in Fig. 3. The spectrum of $\text{Na}_{0.35}\text{CoO}_2 \cdot 1.3\text{H}_2\text{O}$ has two peaks at BEs of 528.6 eV and 531.6 eV. The peak at 528.6 eV is the oxygen $1s$ core level from the CoO_2 layers, as has been observed in layered Co oxides.⁶ The peak at 531.6 eV is ascribed to O $1s$ core level of water, as is evident from its BE.³³ While the 528.6 eV peak is present in $\text{Na}_{0.7}\text{CoO}_2$, the high BE feature at 531.6 eV is missing. A weak intensity feature at a still higher BE of 533 eV is observed, possibly due to carbonate-like contamination which is below the detection limit of x-ray diffraction. The results show that the superconducting sample contains water, which is absent in the nonsuperconducting compound, as expected from the compositions.

The HE-PES VB spectra of $\text{Na}_{0.35}\text{CoO}_2 \cdot 1.3\text{H}_2\text{O}$, $\text{Na}_{0.7}\text{CoO}_2$ and CoO are shown in Fig. 4, along with the soft x-ray ($h\nu = 700$ eV) spectrum of $\text{Na}_{0.35}\text{CoO}_2 \cdot 1.3\text{H}_2\text{O}$. For $\text{Na}_{0.35}\text{CoO}_2 \cdot 1.3\text{H}_2\text{O}$, the HE-PES spectrum shows a low intensity peak at 0.9 eV and a broad structure centered around 6 eV. In comparison, the $h\nu = 700$ eV spectrum shows a higher intensity 0.9 eV peak with the leading edge crossing E_F and a broad peak centered at 5 eV (data normalized at 5 eV BE). The spectral changes for the two photon energies arise from changes in PICS. This is confirmed by comparing the present HE-PES CoO data with that reported in ref. 34 for $h\nu = 600$ eV. The spectral intensity changes and comparison with BSCs (Ref. 35) indicate that the feature at 0.9 eV is due to Co $3d$ states and the broad peak centered

at 5-6 eV is dominated by O $2p$ states. The observed relative intensity changes indicate deviations from available calculated atomic PICS at $h\nu = 8.0$ KeV²⁴ which suggest higher relative intensity of the Co $3d$ states compared to O $2p$ states. BSCs for $\text{Na}_{0.5}\text{CoO}_2$ indicate a peak closer to E_F , with high DOS at E_F derived from Co $3d$ t_{2g} states, which is separated from the Co $3d$ e_g states located in the unoccupied states.³⁵ While oxides can show a contamination peak around 10 eV, the feature at 10.5 eV in CoO is intrinsic as it is observed for cleaved single crystals^{7,34} and in the present case. It is clearly absent in $\text{Na}_{0.7}\text{CoO}_2$. A weak tailing feature between 9-12 eV is observed in $\text{Na}_{0.35}\text{CoO}_2 \cdot 1.3\text{H}_2\text{O}$. Comparing with studies on interaction of water with a high- T_c cuprate³³ and its absence in $\text{Na}_{0.7}\text{CoO}_2$, we attribute it to the water present in $\text{Na}_{0.35}\text{CoO}_2 \cdot 1.3\text{H}_2\text{O}$. But for this feature, the Co $3d$ and O $2p$ derived states are similar in $\text{Na}_{0.35}\text{CoO}_2 \cdot 1.3\text{H}_2\text{O}$ and $\text{Na}_{0.7}\text{CoO}_2$. The VB of CoO shows a feature at nearly 1.6 eV consisting of Co $3d$ states and a higher BE broad feature due to O $2p$ states at about 7 eV. A comparison indicates that in $\text{Na}_{0.35}\text{CoO}_2 \cdot 1.3\text{H}_2\text{O}$ and $\text{Na}_{0.7}\text{CoO}_2$, the Co $3d$ feature is shifted to lower BE compared to CoO, as in Co $2p$ core levels (Fig. 1).

Recent high-resolution ARPES studies on nonsuper-

conducting Na_xCoO_2 ($x = 0.5 - 0.7$) also suggest consistency with BSCs, but with a renormalization of electronic states on a low energy scale of 100 meV.^{13,36} This energy scale is beyond present HE-PES measurements. A more accurate analysis at and very near E_F in superconducting $\text{Na}_{0.35}\text{CoO}_2 \cdot 1.3\text{H}_2\text{O}$ requires higher resolution measurements, preferably with ARPES, to obtain the energy and momentum resolved electronic structure. The interplay of electron-electron correlations and strong electron-phonon coupling³⁷ of renormalized carriers in $\text{Na}_{0.35}\text{CoO}_2 \cdot 1.3\text{H}_2\text{O}$ could stabilize a ‘composite glue’ for pairing, driven by a change in hybridization or intersite Coulomb interactions.

In conclusion, HE-PES provides normal state bulk electronic structure of $\text{Na}_{0.35}\text{CoO}_2 \cdot 1.3\text{H}_2\text{O}$. In contrast to 3-dimensional doped Co oxides, the Co $2p$ core level spectra show well-separated Co^{3+} and Co^{4+} ions. Cluster calculations suggest low spin Co^{3+} and Co^{4+} states, and a moderate on-site $U_{dd} \sim 3\text{--}5.5$ eV. Valence band PES identifies Co $3d$ and O $2p$ derived states, nearly in agreement with BSCs.

AC thanks Professor O. Gunnarsson for very valuable discussions. We thank Drs. M. Arita, T. Tokushima and K. Shimada for valuable experimental support.

-
- ¹ K. Takada et al. Nature 422, 53 (2003)
 - ² J.B. Goodenough, in Progress in Solid State Chemistry, edited by H. Reiss (Pergamon, London, 1971), Vol. 5, p.145 ; M. Imada, A. Fujimori and Y. Tokura, Rev. Mod. Phys. 70, 1039 (1998)
 - ³ J. van Elp, J.L. Wieland, H. Eskes, P. Kuiper, G.A. Sawatzky, F.M.F. de Groot and T.S. Turner, Phys. Rev. B 44, 6090 (1991).
 - ⁴ A. Chainani, M. Mathew and D.D. Sarma, Phys. Rev. B 46, 9976 (1992)
 - ⁵ T. Saitoh, A.E. Bocquet, T. Mizokawa, and A. Fujimori Phys. Rev. B 52, 7934-7938 (1995) ; T. Saitoh et al. Phys. Rev. B 56, 1290 (1997)
 - ⁶ T. Mizokawa et al. Phys. Rev. B 64, 115104 (2001).
 - ⁷ F. Parmigiani and L. Sangaletti, J. Electron Spectrosc. Relat. Phenom. 98-99, 287 (1999).
 - ⁸ A. Fujimori et al., Phys. Rev. B 35, 8814 (1987); Z.-X. Shen et al., *ibid.* 36, 8414 (1987); H. Eskes, L. H. Tjeng, and G. A. Sawatzky, *ibid.* 41, 288 (1990)
 - ⁹ G. Baskaran, Phys. Rev. Lett. 91, 097003 (2003)
 - ¹⁰ B. Kumar and B.S. Shastri, Phys. Rev. B 68, 104508 (2003)
 - ¹¹ Q.-H. Wang, D.-H. Lee, and P. A. Lee, cond-mat/0304377.
 - ¹² W. Koshibae and S. Maekawa, cond-mat/0306696 v1.
 - ¹³ T. Valla et al. Nature 417, 627 (2002)
 - ¹⁴ Y. Wang, N.S. Rogado, R.J. Cava and N.P. Ong, Nature 423, 425 (2003)
 - ¹⁵ R.E. Schaak, T. Klimczuk, M.L. Foo and R.J. Cava, Nature 424, 527 (2003)
 - ¹⁶ J. Kunes, K.-W. Lee and W. Pickett, cond-mat/0308388v1.
 - ¹⁷ I. Terasaki, Physica B 328, 63(2003)
 - ¹⁸ R. Ray, A. Ghoshray, K. Ghoshray and S. Nakamura, Phys. Rev. B 59, 9454 (1999); J.L. Gavilano et al., cond-mat/0308383v1.
 - ¹⁹ J. Zaanen, G. A. Sawatzky and J. W. Allen, Phys. Rev. Lett. 55, 418 (1985).
 - ²⁰ L. Braicovich et al. Phys. Rev. B 56, 15047(1997)
 - ²¹ J. Woicik et al. Phys. Rev. Lett 89, 077401(2002)
 - ²² K. Kobayashi et al., Appl. Phys. Lett. 83, 1005(2003)
 - ²³ NIST Electron Inelastic Mean Free Path Database: Ver 1.1.(2000)
 - ²⁴ J. J. Yeh and I. Lindau, At. Data Nucl. Data Tables 32, 1(1985)
 - ²⁵ I. Lindau, P. Pianetta, S. Doniach and W.E. Spicer, Nature 250, 214(1974)
 - ²⁶ K. Tamasaku, Y. Tanaka, M. Yabashi, H. Yamazaki, N. Kawamura, M. Suzuki, and T. Ishikawa, Nucl. Instrum. Methods A 467/468, 686 (2001).
 - ²⁷ T.E. Kidd, T. Miller and T.-C. Chiang, Phys. Rev. Lett. 83, 2789(1999)
 - ²⁸ P. G. Steeneken et al. Phys. Rev. Lett. 90, 247005 (2003)
 - ²⁹ E.Z. Kurmaev et al. Phys. Rev. B 59, 12799(1999)
 - ³⁰ A.E. Bocquet et al. Phys. Rev. B 45, 1561(1992)
 - ³¹ M. Taguchi, T. Uozumi and A. Kotani. J. Phys. Soc. Jpn. 66, 247 (1997).
 - ³² R. Jin, B.C. Sales, P. Khalifah, and D. Mandrus Phys. Rev. Lett. 91, 217001 (2003)
 - ³³ S.L. Qiu et al., Phys. Rev. B 37, 3747(1988).
 - ³⁴ G. Ghiringhelli et al., Phys. Rev. B 66, 075101(2002).
 - ³⁵ D. J. Singh, Phys. Rev. B 61, 13397(2000) ; 68, 020503(R) (2003).
 - ³⁶ M.Z. Hasan et al. cond-mat/0308438v1; H.-B. Yang et al. cond-mat/0310532v1.
 - ³⁷ O Rosch and O. Gunnarsson. cond-mat/0308035